analytical chemistry

pubs.acs.org/ac Article

Rapid Electrochemical Detection of Bacterial Sepsis in Cirrhotic Patients: A Microscaffold-Based Approach for Early Intervention

Manleen Kaur,[#] Sadam H. Bhat,[#] Rajnish Tiwari, Pratibha Kale, Dinesh M. Tripathi, Shiv Kumar Sarin, Savneet Kaur,[*] and Neetu Singh[*]

Cite This: *Anal. Chem.* 2024, 96, 4925−4932 Read Online

ACCESS | Metrics & More | Article Recommendations | Supporting Information

ABSTRACT: Sepsis is a dysregulated inflammatory response leading to multiple organ failure. Current methods of sepsis detection are time-consuming, involving nonspecific clinical signs, biomarkers, and blood cultures. Hence, efficient and rapid sepsis detection platforms are of utmost need for immediate antibiotic treatment. In the current study, a noninvasive rapid monitoring electrochemical sensing (ECS) platform was developed for the detection and classification of plasma samples of patients with liver cirrhosis by measuring the current peak shifts using the cyclic voltammetry (CV) technique. A total of 61 hospitalized cirrhotic patients with confirmed (culture-positive) or suspected (culture-negative) sepsis were enrolled. The presence of bacteria in the plasma was observed by growth kinetics, and for rapidness, the samples were co-encapsulated in microscaffolds with carbon nanodots that were sensitive enough to detect redox changes occurring due to the change in the pH of the surrounding medium, causing shifts in current peaks in the voltammograms within 2 h. The percentage area under the curve for confirmed infections was 94 and that with suspected cases was 87 in comparison to 69 and 71 with PCT, respectively. Furthermore, the charge was measured for class identification. The charge for LPS-absent bacteria ranged from −400 to −600 μC, whereas the charge for LPS-containing bacteria class ranged from −290 to −300 μC. Thus, the developed cost-effective system was sensitive enough to detect and identify bacterial sepsis.

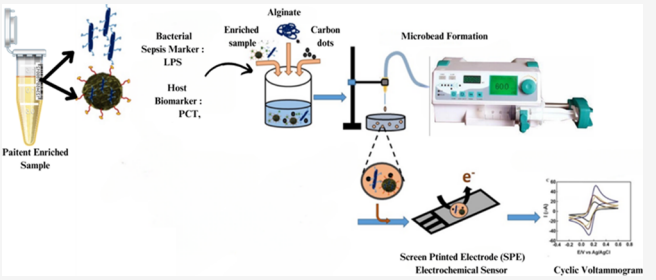

INTRODUCTION

Sepsis is the systemic inflammatory response to an infection. Patients with liver diseases or cirrhosis are the most susceptible to it.[1] Sepsis causes a sudden worsening of liver function in cirrhosis leading to short-term mortality.[2] The existing methods of detection involve blood cultures or biomarker assays. Blood cultures are the gold standard method for bacterial detection but are time-consuming and require large sample volumes, decreasing the sensitivity, and often result in false-negative analysis, making the assay difficult for timely treatment.[3] The biomarkers studied for sepsis such as PCT (procalcitonin), CRP (C-reactive protein), interleukin-6 (IL-6), and tumor necrosis factor-α (TNF-α) are not specific and can also be elevated in other conditions like autoimmune disorders, cancer, obesity, and so forth. PCT is a member of the CAPA protein family. It is a precursor for the hormone calcitonin (CT). The values for PCT are typically less than 0.1 ng/mL in healthy individuals. A significant increase is observed during systemic infections such as sepsis.[4] The clinical usefulness of PCT alone is still not clear because there is no single cutoff value defined for sepsis. Furthermore, the existing studies are single-center observations with many variations in commercialization for clinical setup.[4] CRP is an acute-phase plasma protein synthesized by hepatocytes, and its concentration increases in infections. Healthy plasma has less than or equal to 2 mg/L of CRP. In infections, especially sepsis, the clinical usefulness of CRP alone is still under consideration because of large variations in the chosen cutoff values. Most of the times, the values in the ICU patient sample overlap with those of patients with other causes of inflammation.[4] A combination of elevated serum levels of biomarkers CRP and PCT is considered appropriate for sepsis.[5] Since a delay in antibiotic treatment significantly increases mortality in sepsis patients, timely bacterial detection and antibiotic treatment are crucial.[6,7] Therefore, the need for a rapid, promising, and accurate sepsis diagnostic method has gained the utmost importance.

The researchers have been working for rapid diagnosis and enhanced sensitivity, detecting the low level of presence of bacteria in biological samples. In early stages, at a low bacterial concentration, it is difficult to detect them using the

Received: December 18, 2023
Revised: February 26, 2024
Accepted: February 27, 2024
Published: March 12, 2024

https://doi.org/10.1021/acs.analchem.3c05754
Anal. Chem. 2024, 96, 4925−4932

Table 1. Commercially Available Devices for Sepsis

device	technology	sample	time	disadvantage
StaphPlex[13]	PCR	positive blood culture	5 h after incubation of 24−48 h	time-consuming
Xpert MERSA[14]	PCR	whole blood	1−2 h	large sample volumes
HYPLEX[15]	PCR	positive blood culture	3 h after incubation of 24−48 h	time-consuming
Accuprobe[16]	chemiluminescence	positive blood culture	3 h after incubation of 24−48 h	time-consuming
Verigene[17]	PCR	positive blood culture	3.5 h after incubation of 24−48 h	time-consuming
Film Array[18]	PCR	positive blood culture	1 h after incubation of 24−48 h	time-consuming
Sepsi Test[19]	PCR	whole blood	8−18 h after incubation of 24−48 h	time-consuming
SeptiFast[20]	PCR	positive blood culture	8−10 h after incubation of 24−48 h	larger sample volumes, time-consuming
VYOO[21]	PCR and gel electrophoresis	positive blood culture	6 h after incubation of 24−48 h	larger sample volumes, time-consuming
Magicplex[22]	PCR	positive blood culture	3.5 h after incubation of 24−48 h	time-consuming
T2 bacteria panel[23]	magnetic resonance miniaturized	whole blood	5−8 h after incubation of 24−48 h	time-consuming
Plex-ID BAC[24]	PCR with electrospray ionization	positive blood culture	6 h after incubation of 24−48 h	time-consuming
Quick FISH[25]	fluorescence in situ hybridization	positive blood culture	1.5 h after incubation of 24−48 h	time-consuming
Bactec[26]	automated blood culture	positive blood culture	14−15 h	time-consuming
Virtuo[26]	automated blood culture	positive blood culture	7−10 h	time-consuming

Scheme 1. Schematic Representation of the Platform for Early Bacterial Sepsis Detection

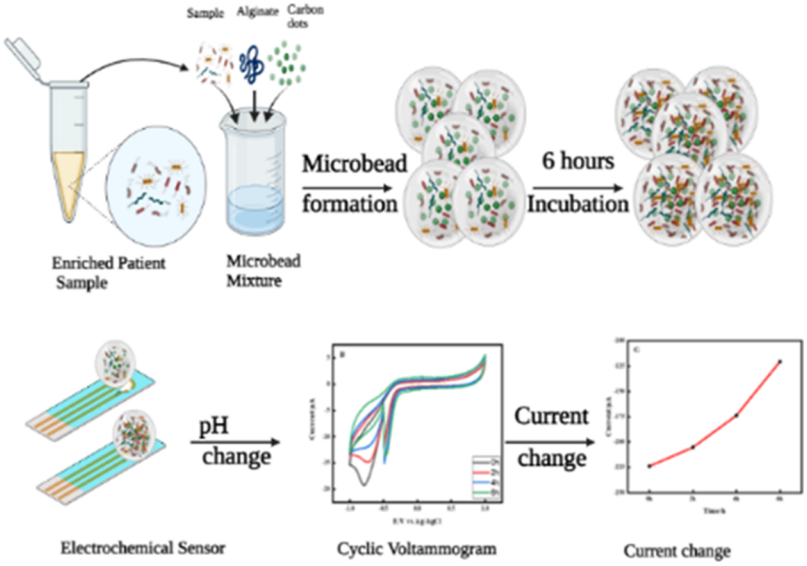

conventional systems as their sensitivity is typically ~10^8 CFU/mL and requires culturing the samples until detectable bacterial concentrations. So far, there is no technique that detects bacterial infection at low concentrations in an early disease stage in less than 24 h.

The techniques to assess bacterial growth depend on different parameters like broth turbidity, pH, and biochemical molecules (O_2, CO_2, and ATP).[8,9] The standard blood-monitoring platforms, prevalent in the market, like Bactec, Vitek, and Sensititer Vizion confirm the bacterial presence in 12−48 h, either by fluorescence spectroscopy or by colorimetric assays.[10−12] The commercially available devices are summarized in Table 1. Interestingly, it is observed that the sensitivity and detection time improve with larger culture vials or an increased sample-to-volume ratio. This observation is not surprising as at high bacterial concentrations the changes in O_2, CO_2, and ATP levels can be easily detected, as the bacterial doubling of few cycles can produce significant changes in smaller volumes. Thus, to push the sensitivity for low sample volumes by increasing the sample-to-culture volume ratio, the culture vials need to be reduced. We hypothesized that a micron-sized culture vial might push the sensitivity to be even higher as a significant number of bacteria occupying the small culture volume can be achieved with lesser doubling cycles, making the detection easy, thus, shortening the detection time. Also, we believe that a microscaffold that allows bacteria to grow easily with a growth detection sensor can be a good alternative.

Bacterial growth can be easily detected with pH changes in the surrounding media over time due to metabolite production (carbonic and lactic acid). This pH change can also result in various redox reactions that can be monitored by cyclic voltammetry (CV). Unlike fluorescence-based sensors, the electrochemical biosensors have become one of the most promising form for developing cost-effective, miniaturized, portable platforms that can be easily integrated with low-cost readout devices.[27]

Recently, we reported a carbon dot (CD)-based microscaffold platform for detecting bacteria using CV.[28] The synthesized CDs help in detecting redox changes due to the change in the pH of the surrounding medium, causing current peak shifts in voltammograms. These micron-sized beads also provided the smaller volume samples with a larger sample-to-volume ratio, creating a microenvironment where the redox

https://doi.org/10.1021/acs.analchem.3c05754
Anal. Chem. 2024, 96, 4925−4932

changes can be detected immediately with CDs in close proximity, making the technique rapid and sensitive.[29] However, the previous platform was not established and calibrated for testing clinically relevant samples, such as blood/plasma. In the current study, improving upon the previous platform, we report a noninvasive and label-free rapid electrochemical bacteria detection platform for bacterial sepsis detection from the liver cirrhosis patient samples (Scheme 1). Also, we were able to classify the bacterial class and perform antibiotic susceptibility testing at low concentrations (up to 100 CFU/mL).

MATERIALS AND METHODS

Synthesis of Carbon Dots and Their Characterization. For CD synthesis, we used the previously reported method with *Agaricus bisporus* and ethylene diamine (1M) as a carbon and nitrogen source, respectively.[30]

The size and surface charge were confirmed by transmission electron microscopy (TEM) and zeta potential, respectively. The electrochemical properties were studied by encapsulating CDs in a microscaffold and incubating for 15 min in an altered pH (5.5 and 7.4) of the nonreducing solution (Hanks' balanced salt solution, HBSS). The CV patterns were recorded after the incubation.

Encapsulation of Biological Samples and CDs in Alginate-Based Microscaffolds. Various bioanalytes like plasma, blood, and protein (bovine serum albumin, BSA) were encapsulated along with CDs in sodium alginate microscaffolds separately. These beads were formulated by mixing alginate (1%) and sodium chloride (NaCl, 0.9%).The solution mixture containing the sample (10 μL/mL) and CDs (0.5 mg/mL) was poured into a 5 mL syringe and dropped into calcium chloride solution for cross-linking by a syringe pump and forming microscaffolds at a defined flow rate of 40 mL/min at a voltage of ∼7000 V.[31] These microscaffolds were incubated for 4 h in HBSS solution at different pH values (5.5 and 7.4) for platform significance.

Encapsulation and Electrochemical Cell Growth Determination of Bacteria Spiked in Healthy Plasma. The initial cell growth study was carried out with bacteria spiked in healthy plasma.

Escherichia coli (*E. coli*) was inoculated in Luria−Bertani (LB, 5 mL) and incubated at 37 °C at 200 rpm overnight (o/n) for primary (1°) culturing. Then, 1% primary was subcultured for 4 h. The absorbance was recorded at 600 nm using a Biotek Synergy H1 microplate reader for cell count. Finally, the different concentrations (10^2 and 10^4 CFU/mL) were spiked in healthy plasma.

To establish that the platform can be used for monitoring bacterial growth, the alginate microscaffolds encapsulated 10 μL/mL of bacteria at different concentrations (10^2 and 10^4 CFU/mL) along with the CDs to mimic clinical samples. The control was healthy plasma co-encapsulating CDs. About 9−10 beads of each sample were taken in a 48-well plate and incubated in HBSS solution in triplicates for 6 h at 37 °C, and CV results were recorded at different time points (0, 2, 4, and 6 h) to monitor changes. We also conducted the experiment without encapsulation in the microscaffold, where 10 μL/mL of spiked plasma (10^2 CFU/mL bacteria spiked in plasma) was mixed in the solution with CDs and 20 μL of the mixture (without microscaffold) was dropped directly on the SPE, and the CV results were recorded at different time points (0, 2, 4, and 6 h) to monitor the current changes.

Electrochemical Studies of Clinical Samples. Plasma samples from patients were collected using the anticoagulant EDTA and centrifuged for 15 min at 1000*g* within 30 min of collection and stored at −20 °C for ECS testing.

The stored plasma (10 μL) was encapsulated along with the CDs (0.5 mg/mL) in microscaffolds. About 9−10 beads of each sample were incubated in HBSS solution in triplicates for 6 h at 37 °C, and the CV results were recorded at different time points (0, 2, 4, and 6 h) for each sample to test positivity.

Validation of the Clinical Samples by Other Bacteria Staining Methods. The microscaffolds were stained with 50 μL of acridine orange (1:1000 dilution) and incubated at room temperature for 15 min, given three HBSS washes, and validated by fluorescence microscopy for the bacterial presence.

Electrochemical Studies for Bacterial Classification. The lipopolysaccharide (LPS) layer in a Gram-negative bacterial membrane differentiates it from a Gram-positive bacteria. To determine if the redox reaction can be used to identify the presence of LPS and hence distinguish between Gram-positive and Gram-negative bacteria, LPS voltammograms of *E. coli* (from Sigma-Aldrich) were recorded by CV. The 5 mg/mL stock was prepared in HBSS, and CV results were recorded at different concentrations (10 μg/mL−1 mg/mL). The charge versus time plot identified the changes in charge with the reduction of LPS.

Further, to identify the charge range for different bacterial classes, microscaffolds were encapsulated with Gram-positive (*S. aureus* and *B. subtilis*) and Gram-negative (*E. coli* and *P. aeruginosa*) bacteria (10 μL/mL). The CV results were recorded for current change, and to observe the net negative charge change with LPS, the charge versus time graph was plotted.

Antibiotic Susceptibility Assay. The bacterial strains (*S. aureus*, *P. aeruginosa*, *K. pneumonia*, and *E. coli*) majorly responsible for sepsis were mixed in equal ratios. The mixture was incubated o/n at 37 °C at 200 rpm in 5 mL of LB media, and 1% inoculum was subcultured for 4 h, and absorbance was recorded. The antibiotic susceptibility assay was performed where microscaffolds co-encapsulated 10^8 CFU/mL mixed bacteria (10 μL/mL), CDs (0.5 mg/mL), and three different antibiotic concentrations (0.5, 2, and 5 mg/mL) depending upon the minimum inhibitory concentration (MIC) of the antibiotics. The antibiotics used for the experiments were amoxycillin and gentamycin.

Statistical Analysis. Statistical analysis was performed on GraphPad Prism 8 software version 8.0.2. Student's unpaired *t* test or Mann−Whitney test was performed to compare two groups depending on the data distribution. $P < 0.05$ was considered significant.

RESULTS AND DISCUSSION

Carbon Dot Characterization. The CDs obtained when characterized were spherical and ∼18 nm in size (Figure S1a) with a charge of −9.84 mV (Figure S1b). Further, the recorded CV patterns at different pH showed a gradual increase in reduction potential with a decrease in pH, suggesting that an acidic environment was beneficial for reduction (Figure S1c).

Electrochemical Studies of Biological Samples in Microscaffolds. To ensure that the platform could be used with biological samples, the CV patterns were observed without the bacteria at different pHs (5.5 and 7.4). As no live bacteria was present in the microscaffold, no pH change

https://doi.org/10.1021/acs.analchem.3c05754
Anal. Chem. 2024, 96, 4925−4932

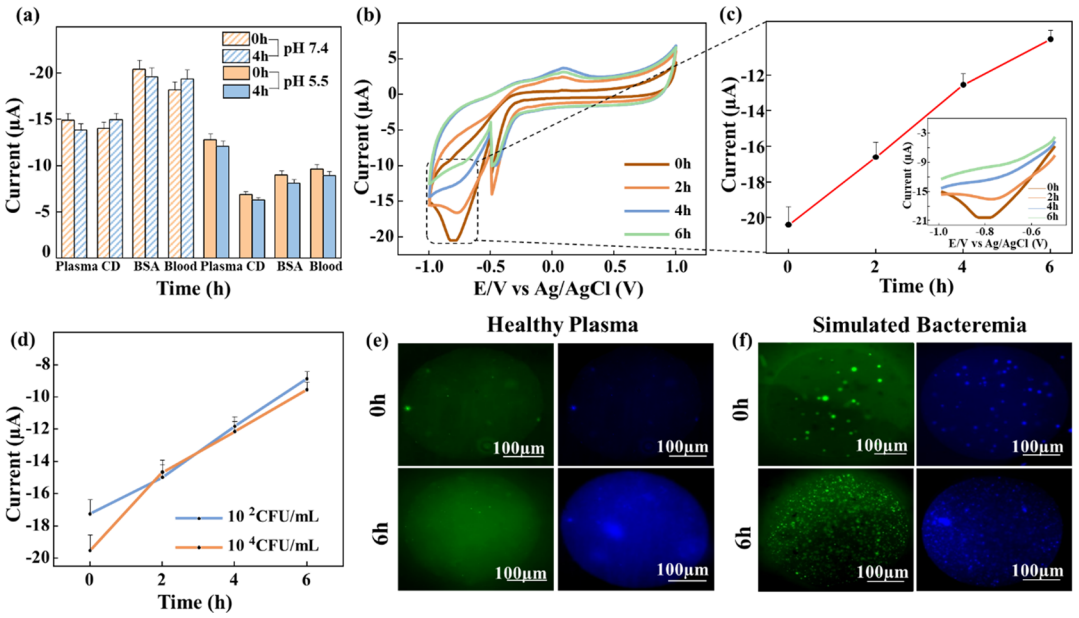

Figure 1. Electrochemical analysis of bacteria-spiked plasma: (a) current change over time of various biological samples (blood, plasma, proteins, and only CDs) at different pH (5.5 and 7.4). (b) Cyclic voltammogram to monitor the bacterial growth in the developed microscaffold platform (alginate scaffold encapsulated with bacteria-spiked plasma and pH-responsive carbon dots). (c) Change in current over time. Inset represents the particular area for current shifts from 0 to 6 h in the range of reduction potential (−1.0 to −0.5 V). (d) Current change observed in different bacterial concentrations over time. Fluorescence microscopy images of microscaffolds encapsulating (e) healthy plasma and (f) simulated bacteria stained with acridine orange (green) and Hoechst (blue).

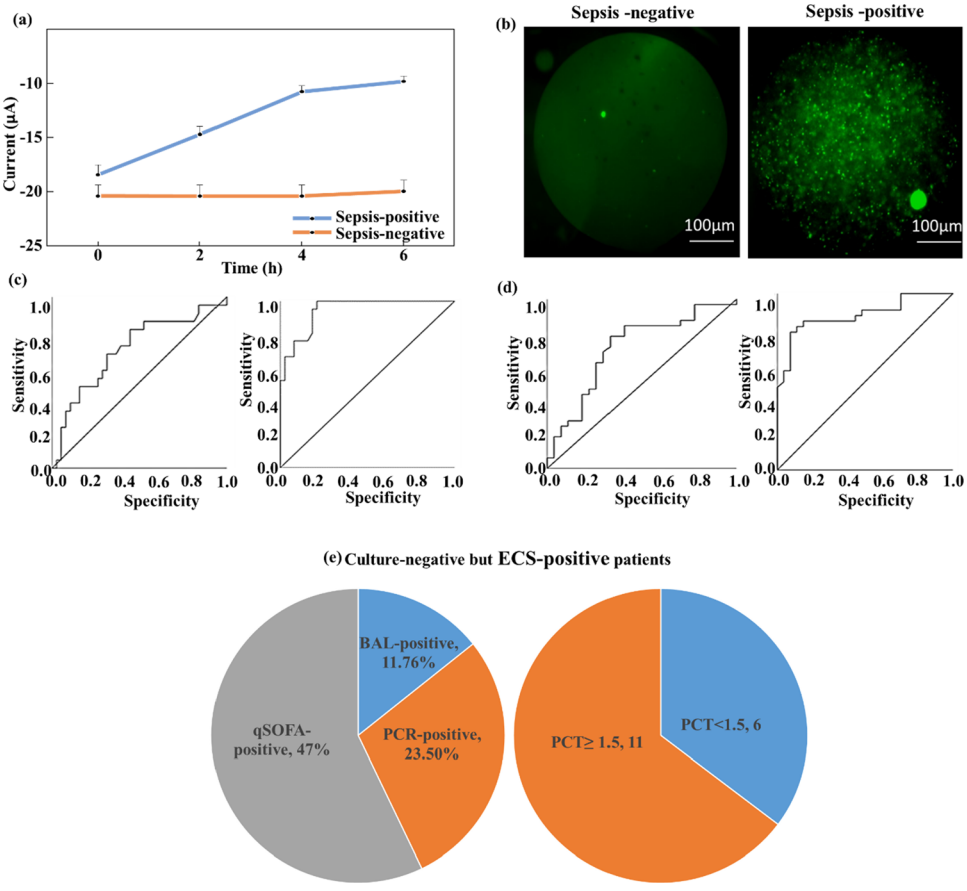

Figure 2. Electrochemical analysis of plasma collected from patients (clinical samples): (a) current change over time in sepsis-negative and sepsis-positive samples. (b) Fluorescence microscopy images of microscaffolds encapsulating samples stained with acridine orange. ROC curves for Epa−Epc and PCT levels for (c) culture-positive infection, (d) sepsis-positivity (either culture or qSOFA), and (e) analysis of culture-negative but ECS-positive samples.

https://doi.org/10.1021/acs.analchem.3c05754
Anal. Chem. 2024, 96, 4925−4932

Scheme 2. Scheme for Classification of Bacteria by Exploiting the Presence and Absence of Cell Wall

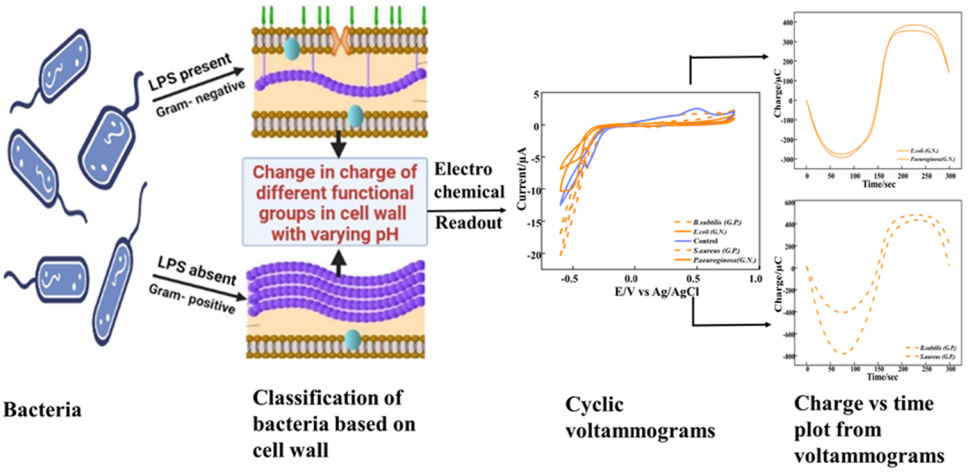

occurred over time, and as a result, no significant change in current was observed (Figure 1a). Further, the bacteria-spiked plasma was co-encapsulated with CDs in the microscaffold to establish a 3D culture platform for bacteria along with the nanosensor that gets ionized on pH changes and provides an optimal microniche for bacterial growth, which was studied by CV. A shift in peaks was observed due to the pH change that occurred with increased bacteria over time (0−6 h). These current shifts when observed for each peak occurred at a fixed reduction potential range (−1.0 to −0.5 V) as seen in Figure 1b, and thus these current peak changes became the readout of the bacterial presence (Figure 1c). The growth of encapsulated bacteria at different concentrations (10^2 and10^4 CFU/mL) was measured by CV to observe the change in current over time (0, 2, 4, and 6 h) (Figure S2a,b). A clear change was observed in the current even with lower concentrations (100 CFU/mL) (Figure S2a), whereas we observed a delayed current change over time with lower concentrations in the nonencapsulated spiked sample when compared to the sample in the encapsulated microscaffolds (Figure S3). Figure 1d shows a significant increase in current over time at different bacterial concentrations (10^2 and 10^4 CFU/mL). Therefore, the limit of detection (LOD) for our system can be defined as 100 CFU/mL in 2 h. With this, we can conclude that the change in current is attributed to the change in pH due to the growth of bacteria over time. Since the CDs are in close proximity to the bacteria and volumes are smaller, it reduces the number of doubling cycles required for observing the changes in pH, enabling fast detection of even minute changes, thus increasing the sensitivity of the platform. These samples were further validated for the presence of bacteria by standard fluorescence microscopy using Hoechst and acridine orange dyes that stain the nucleus of the bacteria (Figure 1e,f).[32]

Electrochemical Studies and Validation of Clinical Samples. After ensuring that the developed platform can be used for biological samples and achieving the limit of detection (LOD) by simulating bacteremia, an enriched clinical plasma sample was studied to establish the 3D microscaffolds for applications in a clinical setting. These samples (10 μL) were co-encapsulated along with the CDs in microscaffolds, and the CV results were recorded at different time points (0, 2, 4, and 6 h) to observe the shifts. As can be seen in Figure S4a, the voltammogram depicts almost no change at the reduction potential peak, thus indicating that the sample encapsulated in the microscaffolds is free from bacterial infection and was defined as a sepsis-negative sample. The same can be seen in the current versus time plots in the fixed reduction potential range. In Figure 2a, there is less electrochemical reactions (oxidation and reduction) occurring, hence leading to no detectable current change for the sepsis-negative sample. However, for sepsis-positive samples, as can be seen in the voltammograms (Figures S4b and 2a current vs time plot), a clear and significant current change occurred when microscaffolds encapsulating the sample were incubated over time. These observations confirmed the feasibility of this noninvasive electrochemical platform as a potential system for early detection (2 h) of bacteria, in lower sample volumes (10 μL), when compared to the gold standard methods for bacterial growth monitoring techniques such as blood culture, which required high bacterial concentration and sample volumes of at least 7−10 mL with culturing time of about 24−72 h.[33] These samples were further confirmed for bacterial presence by fluorescence microscopy using acridine orange, as it stains the nucleus of the bacterial cells (Figure 2b). Since the bacteria was growing in a microscaffold and confined into a small micron region, observing the bacteria by these conventional stains even in low concentrations was easy in comparison to larger standard 2D culture systems. The experiment was repeated for a total of 58 clinical samples, and the CV patterns for each of the sample were recorded along with the validation of the bacteria present in the microscaffolds by visualizing the acridine orange-stained beads by fluorescence microscopy.

Analysis of Culture-Negative but ECS-Positive Patients. The clinical study group and its molecular characterization was done by RT-PCR (Note S1) using designed primers (Table S1). The clinical attributes of culture-positive and -negative sepsis in patients with liver cirrhosis were analyzed (Table S2), and further, for the specificity of the platform, the clinical attributes of the electrochemical sensor (ECS)-positive and -negative sepsis in patients with liver cirrhosis were studied (Table S3). The patient samples that tested negative in culture but gave positive signals in the ECS detection platform were now suspected cases of sepsis and were analyzed by molecular methods. Among the 17 cases that were culture-negative, 8 were qSOFA-positive (47%), 4 were PCR-positive (23.52%), and 2 were culture-positive in BAL (11.76%) (Figure 2e). We next determined the PCT levels of

https://doi.org/10.1021/acs.analchem.3c05754
Anal. Chem. 2024, 96, 4925−4932

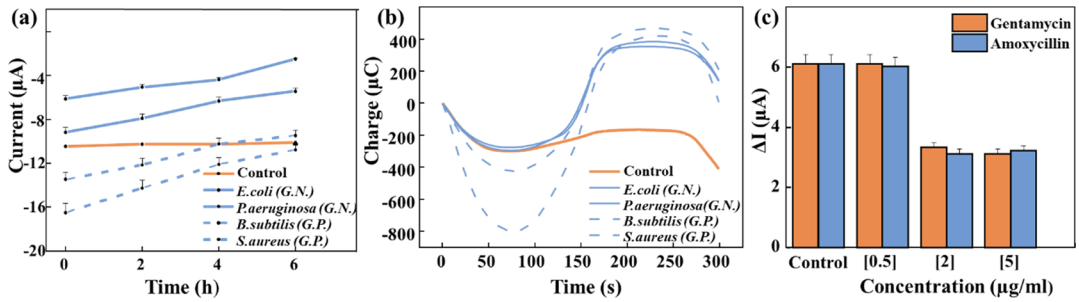

Figure 3. Electrochemical bacterial classification: (a) Current change observed in bacterial classes over time. (b) Charge observed for bacterial strains. (c) Antibiotic susceptibility analysis of spiked plasma.

the 17 suspected cases of sepsis. Out of 17 cases, 11 patients had a higher PCT ≥ 1.5, and in 6 patients, PCT ≤ 1.5 (Figure 2e).

Diagnostic Efficiency of ECS Platform for the Detection of Confirmed Sepsis. To analyze the diagnostic power of the ECS detection system with confirmed infection, we studied receiver operating curves (ROC) using Epa−Epc (6−0 h) values. Epa−Epc (6−0 h) had a high discriminative power for the identification of patients with confirmed culture positivity (AUCROC% = 94.4 [89.2−99.6] as compared to PCT (AUCROC% = 69.2 [54.6−83.8] (Figure 2c). The cutoff values along with the sensitivity and specificity of both Epa−Epc (6−0 h) and PCT levels to identify patients with confirmed infection are given in Table S4.

Diagnostic Efficiency of ECS Platform for the Detection of Confirmed and Suspected Sepsis. The ability of Epa−Epc (6−0 h) values to identify suspected or negative sepsis with a positive qSOFA score was matched. Patients having either culture-positivity, qSOFA score-positivity, or both were taken as sepsis-positive patients and used for ROC analysis.

Epa−Epc (6−0 h) also had a high discriminative power for the identification of patients with sepsis positivity (AUCROC % = 87.8 [78.8−96.7] as compared to PCT (AUCROC% = 71 [57.4−84.6] (Figure 2d). The cutoff values along with the sensitivity and specificity of both Epa−Epc (6−0 h) and PCT levels to identify patients with positive sepsis are given in Table S5.

Bacterial Class Classification and Antibiotic Susceptibility Analysis. The major difference in the two bacterial classes, Gram-negative and Gram-positive, is in the cell membrane composition. We hypothesized that the cell membrane of Gram-negative bacteria that contains LPS might be susceptible to redox reactions due to many ionizable groups on the surface. This redox can be detected by CV and may act as a differentiator of bacterial class[34] (Scheme 2). However, along with LPS, there can be other proteins that can undergo similar redox reactions, but the potential and current characteristics might be different. This would also result in a significant difference in the charge observed on the bacteria or the solution containing it under low pH conditions. To establish this concept, we quantified the charge range of LPS by CV using different concentrations in HBSS. The range obtained for LPS was −200 to −300 μC (Figure S5). To ensure that the developed platform would be beneficial for classifications, initially, the voltammograms at a fixed potential for different biological samples which showed no current change (Figure 1a) even under low pH were further quantified for the charge range. We observed that the blood and control (only CD) microscaffolds showed no significant charge at the reduction potential, or the range is below −200 μC, whereas the healthy plasma and BSA microscaffolds were in the range above −300 μC (Figure S6).

To test the platform for bacterial classification, we used different bacterial strains and recorded the voltammmograms for current and charge change over time (0−6 h) (Figure 3a) and plotted the current versus time and charge versus time plots. Interestingly, the charge range obtained for Gram-negative bacteria (*P. aeruginosa* and *E. coli*) was similar to the range obtained for LPS of −290 to −300 μC (Figure 3b), whereas when observed for Gram-positive bacteria (*S. aureus* and *B. subtilis*), the range was significantly different, about −400 to −600 μC. Thus, this observation clearly suggests that the developed platform can be used for predicting the presence of an LPS-containing (Gram-negative) or non-LPS (Gram-positive) bacterial species simply based on the charge range.

The platform developed can also be used for the rapid analysis of antimicrobial susceptibility and antibiotic screening for bacterial culture. To establish this, we prepared a cocktail of bacteria (a mocking clinical sepsis sample) and subjected it to two antibiotic solutions at concentrations above the minimum inhibitory concentration (MIC). Table S6 represents the electrochemical analysis of the antibiotic treatment of an encapsulated bacterial cocktail in the microscaffold. The current change (ΔI) from 0 to 6 h for antibiotics at a low concentration (0.5 μg/mL) was similar to that of the control (spiked plasma without antibiotic), whereas for concentrations above MIC, the range for ΔI changes. Therefore, this suggests the suitability of the platform for timely (6 h) detection of the antimicrobial susceptibility of the bacteria (10^8 CFU/mL) without delaying the treatment (Figure 3c).

DISCUSSION AND CONCLUSIONS

The electrochemical sensing platform developed in our study detects bacteria in all confirmed cases of sepsis and more significantly in a few culture-negative samples also. This platform co-encapsulated the CDs with patients' plasma samples in microscaffolds and utilized the redox changes in the CV of CDs due to low pH conditions from growing bacteria, causing current peak shifts in voltammograms. The micron-sized beads also provided the samples with a larger sample-to-volume ratio, creating a microenvironment where the plasma sample was in close proximity to the CDs, enabling rapid detection of the bacteria with enhanced sensitivity.[29]

Hence, our platform was sensitive enough to detect samples with low counts of bacteria, which were, however, showing high PCT values and/or later found to be PCR-positive for bacterial species. Interestingly, the ECS-positive cases in our

https://doi.org/10.1021/acs.analchem.3c05754
Anal. Chem. 2024, 96, 4925−4932

study had a significantly higher SOFA score and mortality as compared with ECS-negative cases, indicating the utility of our system to accurately detect sepsis in seriously morbid patients, which otherwise are culture-negative.

Several voltammetric and amperometric sensors have been developed for biomarkers like CRP and PCT detection using labeled nanomaterials.[35,36] Other studies include an EIS-based system for the detection of three biomarkers (PCT, LTA, and LPS) in whole blood samples,[37] microfluidic chips, or microelectrodes for IL-6.[38,39] One study used a microfluidic cell separation system based on CD64, CD69, and CD25 expression for sepsis.[40] These diagnostic tests relied on detecting the sepsis-associated biomarkers using labeled reagents and diluted samples.[41] In our study, we used a 3D microscaffold system encapsulating the lowest undiluted plasma volume, which was beneficial for rapid detection even at the micron volumes. The platform was able to detect and confirm bacteria with the lowest bacterial count (100 CFU/mL) in the plasma sample within 2 h, which was delayed to 6 h without encapsulation (Figure S3). Hence, our label-free platform is one of its kind for early-stage detection which uses pH-sensitive CDs and bacterial growth kinetics to detect bacterial sepsis in low sample volumes. Most importantly, the diagnostic efficiency of our designed platform at cutoff values of 0.141 and 0.075 to diagnose both the confirmed and suspected cases of sepsis, respectively, outperformed the commonly used PCT biomarker. However, its utility to diagnose bacterial infections in patients with cirrhosis, especially in ICU, remains controversial. Different diagnostic thresholds and effectiveness of this marker have been reported in different studies.[42] In liver disease patients, the assessment of serum PCT levels alone may not be enough. In our study subjects, at a cutoff value of 1.73 ng/mL PCT, the sensitivity and specificity for the diagnosis of a confirmed bacterial infection in patients with liver disease were only 66.7 and 65.8%, respectively. Thus, a combination of PCT and testing with our electrochemical sensing platform may prove to be a more reliable test for bacterial sepsis in these patients.

Our platform could also identify the class of bacteria based on LPS as a biomarker for charge difference. The electron movement at a particular current peak shift was used to analyze the charge range for the Gram-positive and Gram-negative bacteria, as shown in a previously performed study.[43] The charge observed in Gram-positive bacteria (*S. aureus* and *B. subtilis*) was in the range of −400 to −600 μC, whereas the charge range for Gram-negative bacteria (*P. aeruginosa* and *E. coli*) was −290 to −300 μC, which was the same as the range of LPS. Our platform also recorded variable current shifts within 6 h when bacterial cultures were treated with antibiotics, suggesting that our platform has the potential for early detection of antimicrobial susceptibility. The overall interval between blood culture collection and a definitive identification and antimicrobial susceptibility result in clinics is 36−48 h. A timely determination is a must to achieve maximum clinical benefits.[44]

In summary, we report a novel noninvasive rapid ECS platform for detection, followed by the classification of bacteria in patients with liver cirrhosis by measuring the reducing potential current peak shifts. The platform is suitable for bedside sepsis detection and has great potential in clinical point-of-care applications.

■ ASSOCIATED CONTENT

Supporting Information

The Supporting Information is available free of charge at https://pubs.acs.org/doi/10.1021/acs.analchem.3c05754.

Additional information for carbon dots' characterization, cyclic voltammogram for spiked bacteria in human plasma, clinical samples, LPS charge, and charge quantification in biological samples; additional experimental details for clinical samples' isolation and characterization; primer designing, clinical attributes, sensitivity, and specificity; and detailed values of electrochemical analysis for antibiotic susceptibility by cyclic voltammetry (PDF)

■ AUTHOR INFORMATION

Corresponding Authors

Savneet Kaur − *Department of Molecular and Cellular Medicine, Institute of Liver and Biliary Sciences, New Delhi 110070, India;* orcid.org/0000-0002-9863-2772; Email: savykaur@gmail.com

Neetu Singh − *Centre for Biomedical Engineering, Indian Institute of Technology, New Delhi 110016, India; Biomedical Engineering Unit, All India Institute of Medical Sciences, New Delhi 110029, India;* orcid.org/0000-0002-7880-4880; Email: sneetu@iitd.ac.in

Authors

Manleen Kaur − *Centre for Biomedical Engineering, Indian Institute of Technology, New Delhi 110016, India*

Sadam H. Bhat − *Department of Molecular and Cellular Medicine, Institute of Liver and Biliary Sciences, New Delhi 110070, India*

Rajnish Tiwari − *Department of Molecular and Cellular Medicine, Institute of Liver and Biliary Sciences, New Delhi 110070, India*

Pratibha Kale − *Department of Microbiology, Institute of Liver and Biliary Sciences, New Delhi 110070, India*

Dinesh M. Tripathi − *Department of Molecular and Cellular Medicine, Institute of Liver and Biliary Sciences, New Delhi 110070, India*

Shiv Kumar Sarin − *Department of Hepatology, Institute of Liver and Biliary Sciences, New Delhi 110070, India*

Complete contact information is available at: https://pubs.acs.org/10.1021/acs.analchem.3c05754

Author Contributions

#M.K. and S.H.B. are equally contributing first authors.

Notes

The authors declare no competing financial interest.

■ ACKNOWLEDGMENTS

We acknowledge the financial support from the Indian Institute of Technology, Delhi. We are grateful to CRF, IITD for TEM facility. We acknowledge the DST TDT/DTB/23/2021 project sponsored by Department of Science and Technology, Govt. of India.

■ REFERENCES

(1) Bajaj, J. S.; Kamath, P. S.; Reddy, K. R. *N. Engl. J. Med.* **2021**, *385* (12), 1151−1152.

(2) Philips, C. A.; Sarin, S. K. *Hepatol Int.* **2016**, *10* (6), 871−882.

(3) Piano, S.; Singh, V.; Caraceni, P.; Maiwall, R.; Alessandria, C.; Fernandez, J.; Soares, E. C.; Kim, D. J.; Kim, S. E.; Marino, M.; et al. *Gastroenterology* **2019**, *156* (5), 1368−1380.e10.
(4) Riedel, S.; Carroll, K. C. *Clin Lab Med.* **2013**, *33* (3), 413−37.
(5) Kibe, S.; Adams, K.; Barlow, G. *J. Antimicrob. Chemother.* **2011**, *66* (Suppl 2), ii33−ii40.
(6) Kumar, S.; Tripathy, S.; Jyoti, A.; Singh, S. G. *Biosens Bioelectron* **2019**, *124*−*125*, 205−215.
(7) Rudd, K. E.; Johnson, S. C.; Agesa, K. M.; Shackelford, K. A.; Tsoi, D.; Kievlan, D. R.; Colombara, D. V.; Ikuta, K. S.; Kissoon, N.; Finfer, S.; et al. *Lancet* **2020**, *395* (10219), 200−211.
(8) Chung, C. Y.; Wang, J. C.; Chuang, H. S. *PLoS One* **2016**, *11* (2), No. e0148864.
(9) Sonderholm, M.; Koren, K.; Wangpraseurt, D.; Jensen, P. O.; Kolpen, M.; Kragh, K. N.; Bjarnsholt, T.; Kuhl, M. *npj Biofilms Microbiomes* **2018**, *4*, 3.
(10) Gottfredsson, M.; Erlendsdottir, H.; Gudmundsson, S. *Antimicrob. Agents Chemother.* **1991**, *35* (12), 2658−61.
(11) Ligozzi, M.; Bernini, C.; Bonora, M. G.; De Fatima, M.; Zuliani, J.; Fontana, R. *J. Clin Microbiol* **2002**, *40* (5), 1681−6.
(12) Rockland, M.; Ruth, M.M.; Aalders, N.; Pennings, L.; Hoefsloot, W.; Wattenberg, M.; van Ingen, J. *J. Clin. Microbiol.* **2019**, *57* (4), No. 10-118, DOI: 10.1128/jcm.01756-18.
(13) Tang, Y. W.; Kilic, A.; Yang, Q.; McAllister, S. K.; Li, H.; Miller, R. S.; McCormac, M.; Tracy, K. D.; Stratton, C. W.; Han, J.; et al. *J. Clin Microbiol* **2007**, *45* (6), 1867−73.
(14) Spencer, D. H.; Sellenriek, P.; Burnham, C. A. *Am. J. Clin Pathol* **2011**, *136* (5), 690−4.
(15) Kaase, M.; Szabados, F.; Wassill, L.; Gatermann, S. G. *J. Clin Microbiol* **2012**, *50* (9), 3115−8.
(16) Bull, T. J.; Shanson, D. C. *J. Hosp Infect* **1992**, *21* (2), 143−9.
(17) Mancini, N.; Infurnari, L.; Ghidoli, N.; Valzano, G.; Clementi, N.; Burioni, R.; Clementi, M. *J. Clin Microbiol* **2014**, *52* (4), 1242−5.
(18) Southern, T. R.; VanSchooneveld, T. C.; Bannister, D. L.; Brown, T. L.; Crismon, A. S.; Buss, S. N.; Iwen, P. C.; Fey, P. D. *Diagn Microbiol Infect Dis* **2015**, *81* (2), 96−101.
(19) Stevenson, M.; Pandor, A.; Martyn-St James, M.; Rafia, R.; Uttley, L.; Stevens, J.; Sanderson, J.; Wong, R.; Perkins, G. D.; McMullan, R.; et al. *Health Technol. Assess* **2016**, *20* (46), 1−246.
(20) Korber, F.; Zeller, I.; Grunstaudl, M.; Willinger, B.; Apfalter, P.; Hirschl, A. M.; Makristathis, A. *Wien Klin Wochenschr* **2017**, *129* (11−12), 427−434.
(21) Marco, F. *Enferm Infecc Microbiol Clin* **2017**, *35* (9), 586−592.
(22) Zboromyrska, Y.; Cilloniz, C.; Cobos-Trigueros, N.; Almela, M.; Hurtado, J. C.; Vergara, A.; Mata, C.; Soriano, A.; Mensa, J.; Marco, F.; et al. *Front. Cell. Infect. Microbiol.* **2019**, *9*, 56.
(23) Nguyen, M. H.; Clancy, C. J.; Pasculle, A. W.; Pappas, P. G.; Alangaden, G.; Pankey, G. A.; Schmitt, B. H.; Rasool, A.; Weinstein, M. P.; Widen, R.; et al. *Ann. Int. Med.* **2019**, *170* (12), 845−852.
(24) Ozenci, V.; Patel, R.; Ullberg, M.; Stralin, K. *Clin Infect Dis* **2018**, *66* (3), 452−455.
(25) Vasala, A.; Hytonen, V. P.; Laitinen, O. H. *Front. Cell. Infect. Microbiol.* **2020**, *10*, 308.
(26) Li, Z.; Liu, S.; Chen, H.; Zhang, X.; Ling, Y.; Zhang, N.; Hou, T. *Acta Clin Belg* **2022**, *77* (1), 71−78.
(27) Molinero-Fernandez, A.; Moreno-GuzmanLopez, M.; Lopez, M.A.; Escarpa, A. *Biosensors* **2020**, *10* (6), 66 DOI: 10.3390/bios10060066.
(28) Das, R.; Singh, N. *Biosens Bioelectron* **2019**, *144*, No. 111640.
(29) Zhang, J.; Shikha, S.; Mei, Q.; Liu, J.; Zhang, Y. *Mikrochim. Acta* **2019**, *186* (6), 361.
(30) Chandra, A.; Singh, N. *ACS Biomater Sci. Eng.* **2017**, *3* (12), 3620−3627.
(31) Chandra, A.; Singh, N. *Chem. Commun. (Camb)* **2018**, *54* (13), 1643−1646.
(32) Francisco, D. E.; Mah, R. A.; Rabin, A. C. *Trans Am. Microsc Soc.* **1973**, *92* (3), 416−21.
(33) Gunsolus, I. L.; Sweeney, T.E.; Liesenfeld, O.; Ledeboer, N.A. *J. Clin. Microbiol.* **2019**, *57* (7), No. 10-1128, DOI: 10.1128/jcm.00425-19.
(34) Jiang, H.; Yang, J.; Wan, K.; Jiang, D.; Jin, C. *ACS Sens* **2020**, *5* (5), 1325−1335.
(35) Li, P.; Zhang, W.; Zhou, X.; Zhang, L. *Clin Biochem* **2015**, *48* (3), 156−61.
(36) Yang, Z. H.; Ren, S.; Zhuo, Y.; Yuan, R.; Chai, Y. Q. *Anal. Chem.* **2017**, *89* (24), 13349−13356.
(37) Panneer Selvam, A.; Prasad, S. *SLAS Technol.* **2017**, *22* (3), 338−347.
(38) Min, J.; Nothing, M.; Coble, B.; Zheng, H.; Park, J.; Im, H.; Weber, G. F.; Castro, C. M.; Swirski, F. K.; Weissleder, R.; et al. *ACS Nano* **2018**, *12* (4), 3378−3384.
(39) Hannah, S.; Addington, E.; Alcorn, D.; Shu, W.; Hoskisson, P. A.; Corrigan, D. K. *Biosens Bioelectron* **2019**, *145*, No. 111696.
(40) Zhou, Y.; Zhang, Y.; Johnson, A.; Venable, A.; Griswold, J.; Pappas, D. *Anal. Chim. Acta* **2019**, *1062*, 110−117.
(41) Papafilippou, L.; Claxton, A.; Dark, P.; Kostarelos, K.; Hadjidemetriou, M. *Adv. Healthc. Mater.* **2021**, *10* (1), 2001378.
(42) Dong, R.; Wan, B.; Lin, S.; Wang, M.; Huang, J.; Wu, Y.; Wu, Y.; Zhang, N.; Zhu, Y. *J. Clin. Transl. Hepatol.* **2019**, *7* (1), 51−55.
(43) Matsunaga, T.; Nakajima, T. *Appl. Environ. Microbiol.* **1985**, *50* (2), 238−42.
(44) Sondhi, P.; Maruf, M. H. U.; Stine, K. J. *Biosensors* **2019**, *10*, 2.

https://doi.org/10.1021/acs.analchem.3c05754
Anal. Chem. 2024, 96, 4925−4932